RECURSIVE MODE MATCHING METHOD FOR MULTIPLE WAVEGUIDE JUNCTION MODELING

Olivier P. Franza and Weng Cho Chew
Electromagnetics Laboratory
Department of Electrical and Computer Engineering
University of Illinois
Urbana, IL 61801

Abstract– The mode matching method is applied to different waveguide geometries, and a recursive scheme is defined to use the appropriate number of modes in each section of the waveguide. Numerical simulations for different types of applications are given and show very good results.

I. INTRODUCTION

A general algorithm has been developed to solve the multiple waveguide junction problem for any arbitrarily shaped hollow waveguide, using the mode matching method in a symbolic matrix formulation. This method is very popular and has already been used in [1], [5], or [6]. Other methods are known for solving the waveguide discontinuity problem: the multimode network representation [2], the finite element method [3], the scattering matrix representation [4], or the recurrence modal analysis [8].

The mode matching method requires that the electric and magnetic fields inside a waveguide be expressed in terms of an infinite sum of its eigenmodes. After having derived such expressions in each waveguide, one applies the boundary conditions at the junction of two different waveguides to match the fields. Hence, one can derive two matrix equations where the reflection and transmission operators are the unknowns, and then solve for them. In the case of a multiple waveguide junction problem, these operators will be derived at each junction, and general operators will be defined for the entire structure.

The problem of the accuracy in the results is mainly due to the order of truncation of the infinite expansion needed for the fields. We define a condition on the number of modes in each section of the waveguide that gives good precision in the recursive process, whose accurate results are shown using numerical simulations.

II. THE MODE MATCHING METHOD THEORY

We present the basic formulations of the mode matching method in the general case of an arbitrarily shaped hollow waveguide. We will first recall the expressions obtained in the case of a single junction, as they can be found in [9], and then derive from the equations the expressions of the complete structure's reflection and transmission operators for a double junction and multiple waveguide junctions.

Single waveguide Junction

The fields have to be expanded in terms of the eigenmodes of the waveguide. For the z-component, they can be written as

$$H_z = \sum_i H_i \psi_{hi}(\mathbf{r}_s) e^{ik_{hiz}z} \qquad \text{(for TE modes)} \tag{1}$$

$$E_z = \sum_i E_i \psi_{ei}(\mathbf{r}_s) e^{ik_{eiz}z} \qquad \text{(for TM modes)} \tag{2}$$

where $\psi_{hi}(\mathbf{r}_s)$ and $\psi_{ei}(\mathbf{r}_s)$ are the solutions to the wave equation $(\nabla_s^2 + k^2 - k_{iz}^2)\psi_i(\mathbf{r}_s) = 0$ in two dimensions, with Neumann and Dirichlet boundary conditions, respectively. Once the z-components of the eigenvectors are known, the transverse components can be easily derived using Maxwell's equations

$$\mathbf{E}_s = \sum_i \left[\frac{E_i}{k_{eis}^2} i k_{eiz} \nabla_s \psi_{ei}(\mathbf{r}_s) e^{ik_{eiz}z} - \frac{i\omega\mu H_i}{k_{his}^2} \hat{z} \times \nabla_s \psi_{hi}(\mathbf{r}_s) e^{ik_{hiz}z} \right] \tag{3}$$

$$\mathbf{H}_s = \sum_i \left[\frac{i\omega\epsilon E_i}{k_{eis}^2} \hat{z} \times \nabla_s \psi_{ei}(\mathbf{r}_s) e^{ik_{eiz}z} + \frac{H_i}{k_{his}^2} i k_{hiz} \nabla_s \psi_{hi}(\mathbf{r}_s) e^{ik_{hiz}z} \right] \tag{4}$$

where $k_{eis}^2 = k^2 - k_{eiz}^2$ and $k_{his}^2 = k^2 - k_{hiz}^2$.

As shown in [9], after rearranging the terms into two groups, one for the TE and one for the TM modes, Equations (3) and (4) become

$$\mathbf{E}_s = \mathbf{\Psi}^t(\mathbf{r}_s) \cdot e^{i\,\mathbf{K}z} \cdot \mathbf{e} \tag{5}$$

$$\hat{z} \times \mathbf{H}_s = -\,\mathbf{\Psi}^t(\mathbf{r}_s) \cdot \mathbf{G} \cdot e^{i\,\mathbf{K}z} \cdot \mathbf{e} \tag{6}$$

Then, we define

$$\mathbf{D}_i = \left\langle \mathbf{\Psi}_i,\ \mathbf{\Psi}_i^t \right\rangle = \int_{S_a} dS \mathbf{\Psi}_i(\mathbf{r}_s).\mathbf{\Psi}_i^t(\mathbf{r}_s) \tag{7}$$

$$\mathbf{L}_{ia} = \left\langle \ \mathbf{\Psi}_i, \ \mathbf{\Psi}_a^t \right\rangle = \int\limits_{S_a} dS \mathbf{\Psi}_i(\mathbf{r}_s).\mathbf{\Psi}_a^t(\mathbf{r}_s) \tag{8}$$

so that we can derive from the boundary conditions a set of expressions for the operators $\mathbf{R}$ and $\mathbf{T}$ (see [10]):

$$\mathbf{R} = \ \mathbf{D}_1^{-1} : \mathbf{L}_{1a} \cdot \ (\mathbf{L}_{1a}^t : \mathbf{G}_1 : \mathbf{D}_1^{-1} : \mathbf{L}_{1a} + \mathbf{L}_{2a}^t : \mathbf{G}_2 : \mathbf{D}_2^{-1} : \mathbf{L}_{2a} \ )^{-1} \cdot 2 \ \mathbf{L}_{1a}^t : \mathbf{G}_1 - \mathbf{I} \tag{9}$$

and

$$\mathbf{T} = \ \mathbf{D}_2^{-1} : \mathbf{L}_{2a} \cdot (\mathbf{L}_{1a}^t : \mathbf{G}_1 : \mathbf{D}_1^{-1} : \mathbf{L}_{1a} + \mathbf{L}_{2a}^t : \mathbf{G}_2 : \mathbf{D}_2^{-1} : \mathbf{L}_{2a} \ )^{-1} \cdot 2 \ \mathbf{L}_{1a}^t : \mathbf{G}_1 \tag{10}$$

Double Waveguide Junction

In this case, the electric field in the first waveguide can be written with a generalized reflection operator, as those defined in [10] for layered media, $\widetilde{\mathbf{R}}_{12}$:

$$\mathbf{E}_{1s} = \ \mathbf{\Psi}_1^t(\mathbf{r}_s) \cdot (e^{i \ \mathbf{K}_1 z} + e^{-i \ \mathbf{K}_1 z} \cdot \ \widetilde{\mathbf{R}}_{12}) \cdot \mathbf{e} \tag{11}$$

In the second waveguide, as shown in Figure 1a, we will write the solution as a superposition of waves travelling in two directions

$$\mathbf{E}_{2s} = \ \mathbf{\Psi}_2^t(\mathbf{r}_s) \cdot (e^{i \ \mathbf{K}_2 z} \cdot \mathbf{A}_2 + e^{-i \ \mathbf{K}_2 z} \cdot \mathbf{B}_2) \tag{12}$$

In the third waveguide, an expression similar to the one derived in Equation (15) can be written

$$\mathbf{E}_{3s} = \ \mathbf{\Psi}_3^t(\mathbf{r}_s) \cdot e^{i \ \mathbf{K}_3 z} \cdot \mathbf{A}_3 \tag{13}$$

All of the coefficients, $\mathbf{A}_2$, $\mathbf{B}_2$, and $\mathbf{A}_3$, can be found by again applying matching conditions with physical insight [10]. They finally lead to the expression of the generalized reflection and transmission coefficients

$$\widetilde{\mathbf{R}}_{12} = \ \mathbf{R}_{12} + \ \mathbf{T}_{21} \cdot e^{i \ \mathbf{K}_2 (h_2 - h_1)} \cdot \ \mathbf{R}_{23} \cdot e^{i \ \mathbf{K}_2 (h_2 - h_1)} \cdot (\ \mathbf{I} - \ \mathbf{R}_{21} \cdot e^{i \ \mathbf{K}_2 (h_2 - h_1)} \cdot \mathbf{R}_{23} \cdot e^{i \ \mathbf{K}_2 (h_2 - h_1)})^{-1} \cdot \ \mathbf{T}_{12} \tag{14}$$

These intermediate results are now applied to the multiple waveguide junction problem.

Multiple Waveguide Junction

By analogy with the double waveguide junction problem, the following expressions for the field in waveguide j, the generalized reflection operator

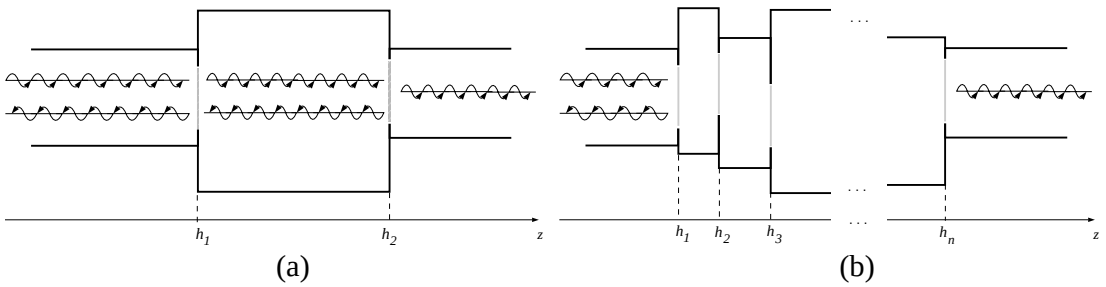

Figure 1 (a) Double junction and (b) multiple junction

$\widetilde{\mathbf{R}}_{j,j+1}$, and the amplitude $\mathbf{A}_j$, can be derived in the case of an N waveguide junction, as shown in Figure 1b.

$$\mathbf{E}_{js} = \mathbf{\Psi}_j^t(\mathbf{r}_s) \cdot (e^{i\,\mathbf{K}_j z} + e^{-i\,\mathbf{K}_j(z-h_j)} \cdot \widetilde{\mathbf{R}}_{j,j+1} \cdot e^{i\,\mathbf{K}_j h_j}) \cdot \mathbf{A}_j \tag{15}$$

$$\widetilde{\mathbf{R}}_{j,j+1} = \mathbf{R}_{j,j+1} + \mathbf{T}_{j+1,j} \cdot e^{i\,\mathbf{K}_{j+1}(h_{j+1}-h_j)} \cdot \widetilde{\mathbf{R}}_{j+1,j+2} \cdot e^{i\,\mathbf{K}_{j+1}(h_{j+1}-h_j)}$$
$$\cdot \Big[\, \mathbf{I} - \mathbf{R}_{j,j+1} \cdot e^{i\,\mathbf{K}_{j+1}(h_{j+1}-h_j)} \cdot \widetilde{\mathbf{R}}_{j+1,j+2} \cdot e^{i\,\mathbf{K}_{j+1}(h_{j+1}-h_j)} \Big]^{-1} \cdot \mathbf{T}_{j,j+1} \tag{16}$$

and

$$\mathbf{A}_j = e^{-i\,\mathbf{K}_j h_{j-1}} \cdot \left(\mathbf{I} - \mathbf{R}_{j,j-1} \cdot e^{i\mathbf{K}_j(h_j - h_{j-1})} \cdot \widetilde{\mathbf{R}}_{j,j+1} \cdot e^{i\mathbf{K}_j(h_j - h_{j-1})} \right)^{-1}$$
$$\cdot \mathbf{T}_{j-1,j} \cdot e^{i\mathbf{K}_{j-1} h_{j-1}} \cdot \mathbf{A}_{j-1} \tag{17}$$

or, in a more compact form,

$$\mathbf{A}_j = \mathbf{S}_{j-1,j} \cdot \mathbf{A}_{j-1} \tag{18}$$

With these recursive equations, an algorithm which finds the expression of the field everywhere in the waveguide, and the generalized reflection and transmission operators of any structure composed of arbitrarily shaped waveguides, can be implemented. The reflection and transmission operators of the entire set of discontinuities are defined by the following

$$\widetilde{\mathbf{R}} = \widetilde{\mathbf{R}}_{1,2} \tag{19}$$

$$\widetilde{\mathbf{T}} = \mathbf{T}_{N-1,N} \cdot \mathbf{S}_{N-2,N-1} \cdots \mathbf{S}_{1,2} \tag{20}$$

The expressions of the reflection and the transmission operators have been derived, with no loss of generality; we just considered a series of circular hollow

waveguides. The only problem is that the mode matching method requires in theory an infinite series expansion of the fields. In the numerical implementation, we will have to truncate the expansion of the fields; the choice of the number of modes is very difficult. One solution is to determine numerically, by trial-and-error, the minimum number of modes needed in the three expansions (Ψ_1, Ψ_2, and Ψ_a). But there are also methods in the literature that give conditions on these numbers. Therefore, a recursive scheme can be deduced to find them; in fact, it would have been impossible to do it numerically in the case of a multiple waveguide junction.

III. OPTIMIZATION OF THE TRUNCATION PROBLEM

The main problem of the mode matching method is the determination of the number of modes necessary to obtain an accurate result. It can be shown by integral equation formulation [10], if N is large enough, that the following relations have to be satisfied:

$$\frac{P_1}{d_1} > \frac{N}{d_a}, \qquad \frac{P_2}{d_2} > \frac{N}{d_a}, \qquad \frac{P_1}{d_1} \simeq \frac{P_2}{d_2} \tag{21}$$

where P_i is the number of modes in region i, N is the number of modes on the diaphragm, d_i is the size of waveguide i, and d_a is the size of the diaphragm.

In the case of a rectangular waveguide, we defined $P_{x,i}$, $P_{y,i}$, N_x and N_y as the number of modes in the x- or y-directions. In each direction, Equation (21) needs to be satisfied. Our numerical results show that for $N \simeq 24$, the values obtained for the TE_{10} reflection coefficient are very good. This represents approximately four modes in each direction. For multiple waveguide junctions, we use the following equations to find the number of required modes. In the case of a rectangular waveguide, in the x- and y-directions,

$$\frac{P_{x,1}}{a_1} = \frac{P_{x,2}}{a_2} = \frac{N_x}{a_a}, \qquad \frac{P_{y,1}}{b_1} = \frac{P_{y,2}}{b_2} = \frac{N_y}{b_a} \tag{22}$$

In the case of a circular waveguide, in the ρ- and ϕ-directions,

$$\frac{P_{\rho,1}}{a_1} = \frac{P_{\rho,2}}{a_2} = \frac{N_\rho}{a_a}, \qquad \frac{P_{\phi,1}}{a_1} = \frac{P_{\phi,2}}{a_2} = \frac{N_\phi}{a_a} \tag{23}$$

Equations (22) and (23) are similar to Equation (21), but are applied to each dimension of the waveguide section, because these dimensions (x and y for the rectangular case, ρ and ϕ in the circular case) are independent of each other

in the basis expansion. The process is repeated for each new junction, using the preceding values.

IV. NUMERICAL RESULTS

This section shows numerical results in comparison to those found in the literature. We will consider complex geometries with ten or more discontinuities. They show the capability of the waveguide junction modeling theory and its applications.

The circular waveguide filter example has been taken from [5], and our results show very good agreement. The geometry of the structure (see Figures 2 and 3) is such that the waveguide operates as a filter for a certain range of frequencies, that are only determined by the geometry of the waveguides, as shown on Figure 4. The case of the corrugated waveguide polarizer has been checked with [6] and [7] and shows good agreement. The symmetric geometry is given in Figure 5, where $d(z)$ is known as the profile function and defines the slot depth of the discontinuities. The example analyzed here uses a linear profile function, which enables us to obtain the slot depths defined in Table 1a. We consider 30 discontinuities for different dominant modes in three different cases. The first case is for a square waveguide geometry, which means that the geometry is the same in the x- and y-directions, and the results are shown on Figure 6, where the gain is defined by $\mathbf{G}_{dB} = 20 \log \mathbf{R}$. For the results of Figure 7, we considered a rectangular waveguide geometry, which means that in the y-direction, the size of the waveguide is constant. Finally we used a circular geometry, whose results are shown in Figure 8. One of the properties of this kind of waveguide structure is that the differential phase shift $\Delta\phi$ between two similar modes (TE_{01} and TE_{11} for instance) is continuous as a function of the frequency as shown on Figure 9, where the horizontal lines show the 90^o ($\pm 2^o$) phase shift area.

Three low-pass filters are finally considered and show good agreement with [1]. The first waveguide filter considered is rectangular. Its geometry is given in Figure 10. The example analyzed here is an array of capacitive step that becomes a low-pass filter device. The structure has 28 discontinuities; their lengths are presented in Table 1b. From Figure 11, we can see that the structure is acting as a low-pass filter for the TE_{10} mode. Ten new elements are added to the structure, as shown in Figure 12. The result is given in Figure 13, where

it can be seen that the second structure has a slightly higher cut-off frequency. Finally, the simpler structure of Figure 14, with circular waveguide elements, gives the results shown in Figures 15 and 16. We also show the phase of the reflection coefficient of some modes in Figure 17. On the range of frequency [8.0 GHz, 13.0 GHz], the structure behaves as a phase shifter for most of the modes.

Table 1 Corrugated waveguide slot depths (a) and low-pass filter lengths (b)

(a)

Quantity	Size in mm
a	17.997
b	17.997
e	3.720
t	0.942
d_1	0.279
d_2	0.513
d_3	0.746
d_4	0.980
d_5	1.214
d_6	1.447
d_7	1.681
d_8	1.914

(b)

Quantity	Size in mm
a	19.05
b_1	19.05
b_2	16.62
b_3	14.18
b_4	11.75
b_5	9.32
b_6	8.11
b_7	21.48
l_1	1.94
l_2	3.72
l_3	4.51

V. CONCLUSIONS

This very powerful method of multiple waveguide junction analysis can be very accurate. The number of unknowns needed (the number of modes) is not too large ($N \approx 24$ for the rectangular case, $N \approx 30$ for the circular case). The complexity of the algorithm is then $\mathcal{O}(MN^3)$, where M is the number of discontinuities. For each iteration, we have to compute four dense reflection and transmission matrices, which require one matrix inversion and four multiplications. We are presently working on the improvement of the storage and the computation of the matrices, and expect to reduce the complexity to $\mathcal{O}(MN^2)$.

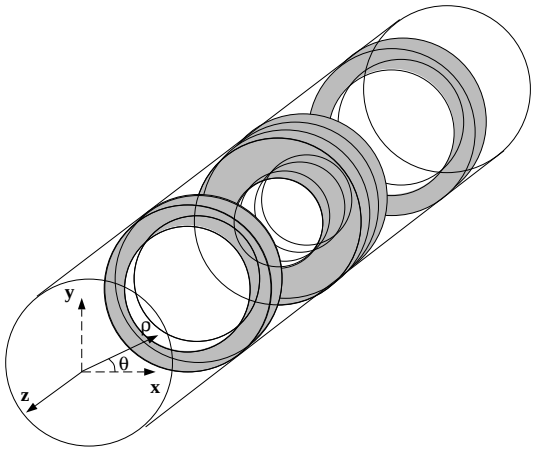

Figure 2 Geometry of the circular waveguide stopband filter

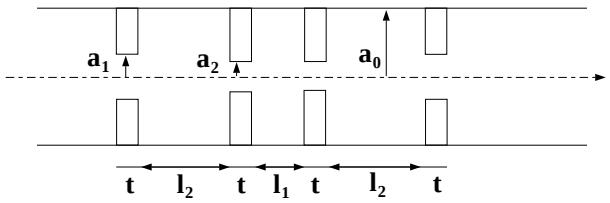

a_0 = 16.269 mm	t = 0.2 mm
a_1 = 6.718 mm	l_1 = 10.907 mm
a_2 = 3.888 mm	l_2 = 11.142 mm

Figure 3 Numerical lengths of the circular waveguide stopband filters

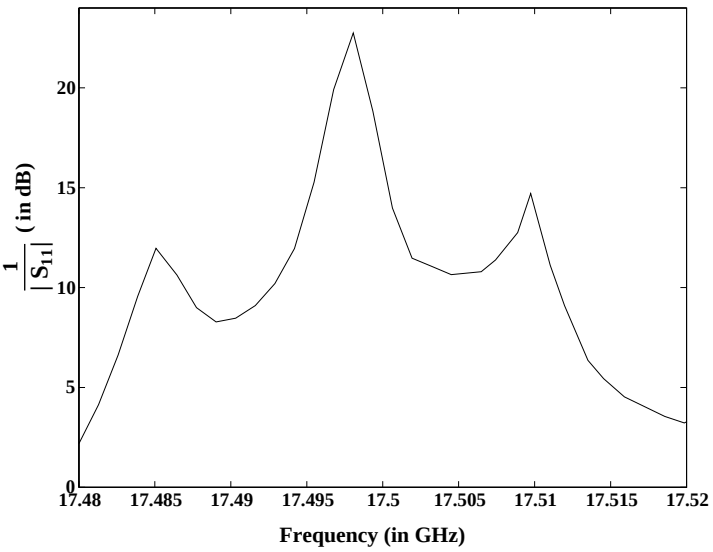

Figure 4 Return loss of the circular waveguide filter, with its three stopband poles

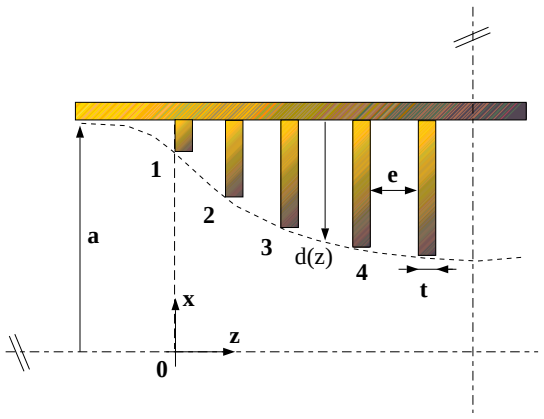

Figure 5 Geometry of a profiled depth corrugated waveguide polarizer

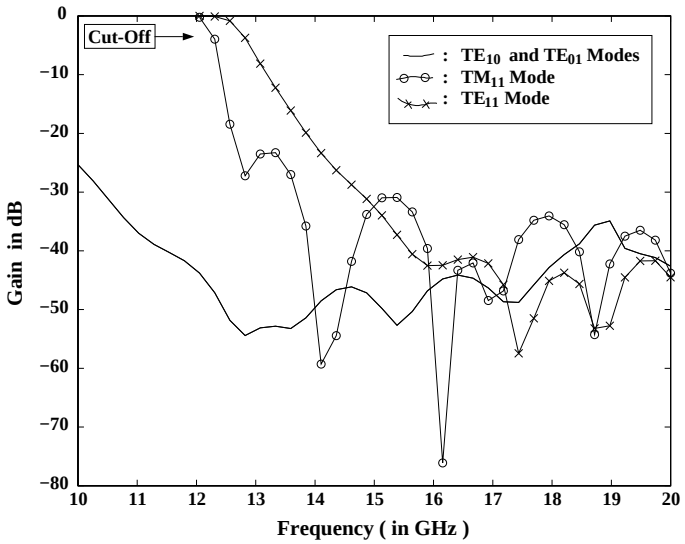

Figure 6 Gain of different waveguide modes
for the corrugated square waveguide polarizer

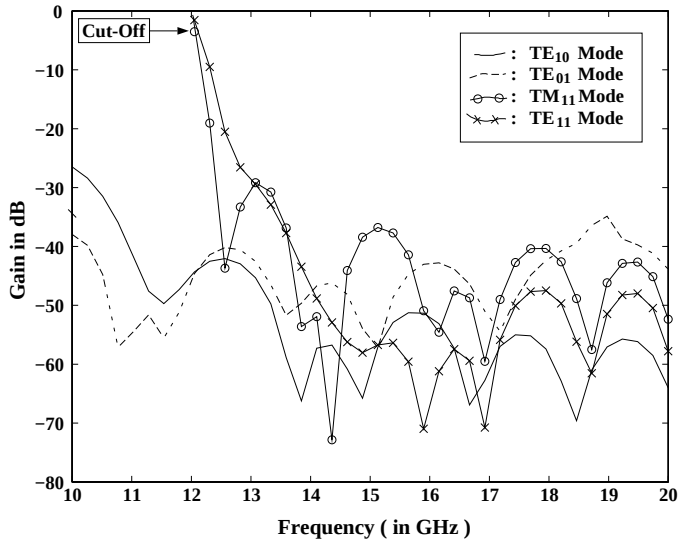

Figure 7 Gain of different waveguide modes
for the corrugated rectangular waveguide polarizer

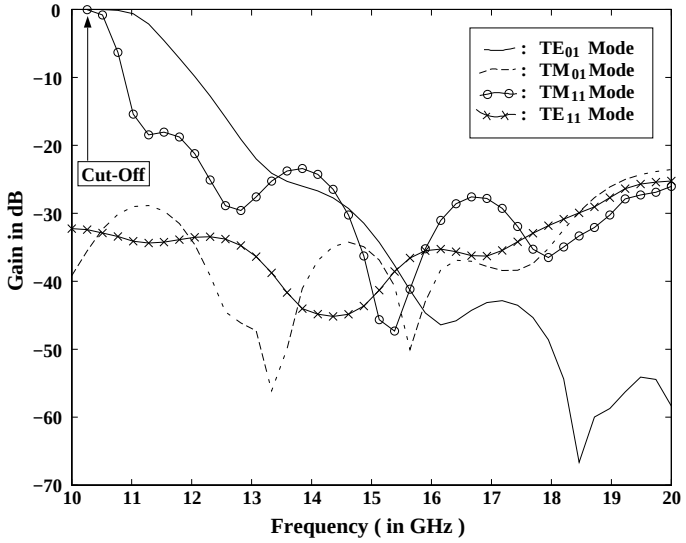

Figure 8 Gain of different waveguide modes for the corrugated circular waveguide polarizer

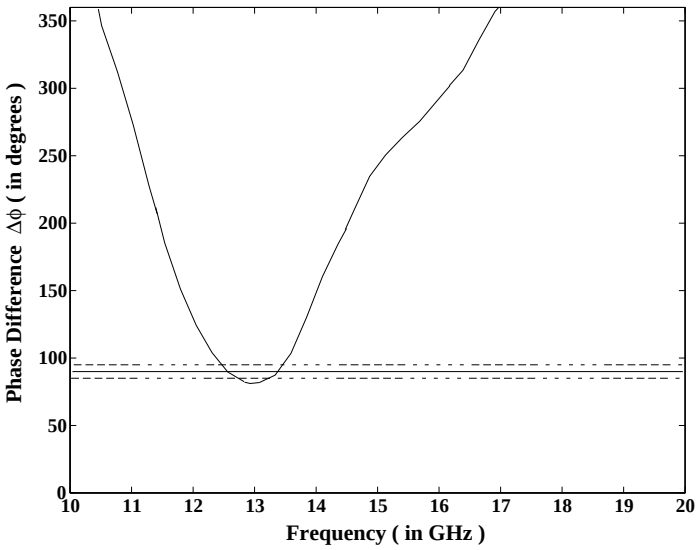

Figure 9 Difference of phase between the TE_{01} and TE_{11} modes for the corrugated circular waveguide polarizer

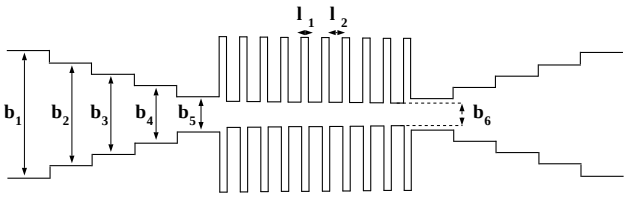

Figure 10 Geometry of the first low-pass filter

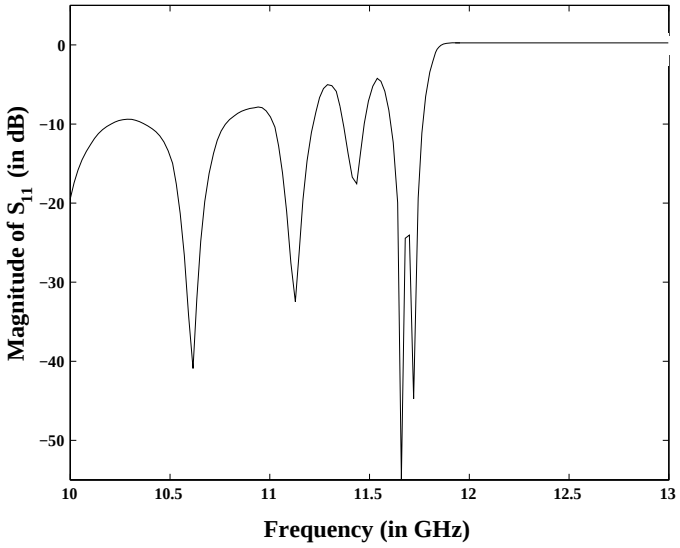

Figure 11 Magnitude of S_{11} for the first low-pass filter

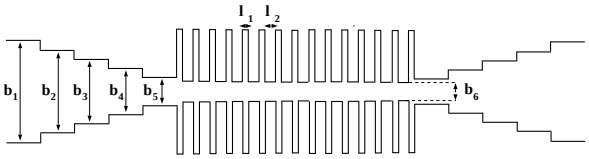

Figure 12 Geometry of the second low-pass filter

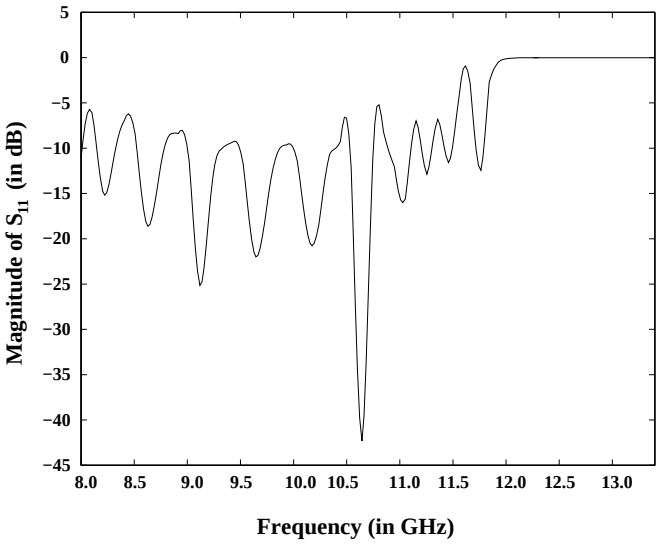

Figure 13 Magnitude of S_{11} for the second low-pass filter

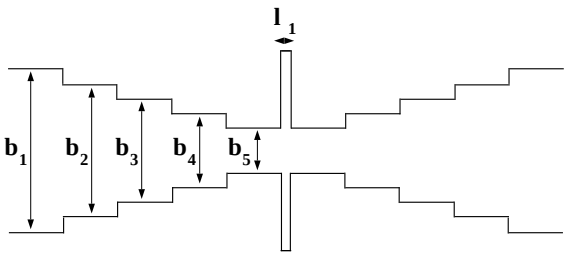

Figure 14 Geometry of the third low-pass filter

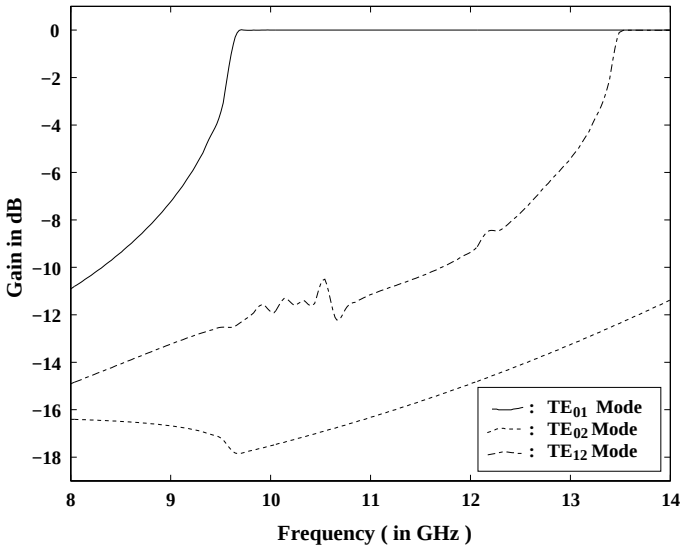

Figure 15 Gain of some TE modes of the third low-pass filter

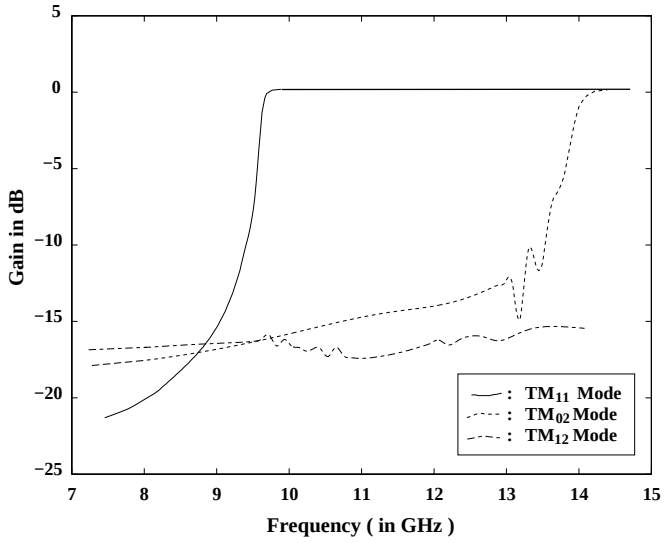

Figure 16 Gain of some TM modes of the third low-pass filter

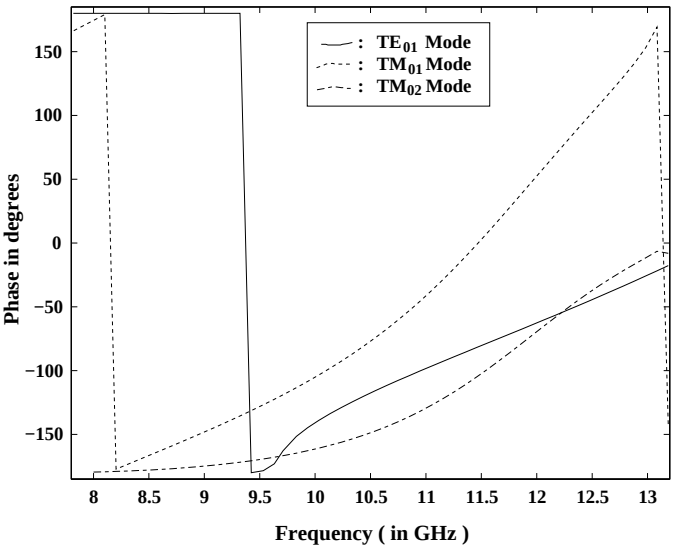

Figure 17 Phase of some modes of the third low-pass filter

REFERENCES

[1] J. Bornemann and R. Vahldieck,"Characterization of a class of waveguide discontinuities using a modified TE^x_{mn} mode approach," *IEEE Transactions on Microwave Theory and Techniques*, vol. 38, no. 12, pp. 1816-1822, Dec. 1990.

[2] M. Guglielmi and G. Gheri,"Rigourous multimode network representation of capacitive steps," *IEEE Transactions on Microwave Theory and Techniques*, vol. 42, no. 4, pp. 622-628, April 1994.

[3] G. M. Wilkins, J.-F. Lee and R. Mittra,"Numerical modeling of axisymmetric coaxial waveguide discontinuities," *IEEE Transactions on Microwave Theory and Techniques*, vol. 39, no. 8, pp. 1323-1328, Aug. 1991.

[4] A. S. Omar and K. Schunemann,"Transmission matrix representation of finline discontinunities," *IEEE Transactions on Microwave Theory and Techniques*, vol. MTT-33, no. 9, pp. 765-770, Sep. 1985.

[5] U. Papziner and F. Arndt,"Field theoretical computer-aided design of rectangular and circular iris coupled rectangular or circular waveguide cavity filters," *IEEE Transactions on Microwave Theory and Techniques*, vol. 41, no. 3, pp. 462-471, March 1993.

[6] U. Tucholke and F. Arndt,"Field theory design of square waveguide iris polarizer," *IEEE Transactions on Microwave Theory and Techniques*, vol. MTT-34, no. 1, pp. 156-160, Jan. 1986.

[7] G. L. James,"Analysis and design of TE_{11} -to- HE_{11} corrugated cylindrical waveguide mode converters," *IEEE Transactions on Microwave Theory and Techniques*, vol. MTT-29, no. 10, pp. 1059-1066, Oct. 1981.

[8] G. A. Gesell and I. R. Ciric,"Recurrence modal analysis for multiple waveguide discontinuities and its application to circular structures," *IEEE Transactions on Microwave Theory and Techniques*, vol. 41, no. 3, pp. 484-490, March 1993.

[9] W. C. Chew, K. H. Lin, J. Friedich and C. H. Chan,"Reflection and transmission operators for general discontinuities in waveguides," *Journal of Electromagnetic Waves and Applications*, vol. 5, no. 8, pp. 819-834, 1991.

[10] W. C. Chew, *Waves and Fields in Inhomogeneous Media.* New York: Van Nostrand Reinhold, 1990.